ChemComm

View Article Online / Journal Homepage / Table of Contents for this issue
Dynamic Article Links

Cite this: *Chem. Commun.*, 2011, **47**, 8928–8930

www.rsc.org/chemcomm

COMMUNICATION

An *all-organic* steroid–D–π-A modular design drives ferroelectricity in supramolecular solids and nano-architectures at RT†

Deepak Asthana,[a] Anil Kumar,[b] Abhishek Pathak,[c] Pradip Kumar Sukul,[d] Sudip Malik,[d] Ratnamala Chatterjee,[c] Satyabrata Patnaik,[b] Kari Rissanen[e] and Pritam Mukhopadhyay*[a]

Received 25th April 2011, Accepted 24th May 2011
DOI: 10.1039/c1cc12398j

Confluence of a modular design approach and self-assembly with a '*steroid–D–π-A*' module generates spontaneous polarization in solids and for the first time in nano-architectures constituted from organogels, at room temperature (RT).

The search for novel ferroelectric (FE) materials has attracted tremendous interest due to the exciting applications in FE random-access memories (FERAM), FE field effect transistors (FEFET), FE diodes, 1-D FE organic quantum magnet and multiferroic materials.[1] By definition, FEs are polar materials in which the spontaneous electric polarization can be reversed by inverting the applied external electric field. FE materials have been dominated by inorganic compounds, which suffer from inability towards solution processing, high temperature for sample preparation, high electric coercive field (E_c) and hazards related to metal ion toxicity.[2] On the other hand, all-organic FE materials should provide multi-fold advantages such as synthetic tailorability, tunability of molecular interactions and solution processing.

Since the discovery of Rochelle Salt, the first FE material with an organic component way back in 1921,[3a] surprisingly a very few all-organic single-component (AOSC) FE solid materials have been reported up to now.[3] The discovery of AOSC FE materials have been accidental and clear-cut design strategies are yet to evolve. In general, existing AOSC FE materials suffer from very low saturation and remnant electric polarization (P_s and P_r of the order of 10^{-9} C cm^{-2}), high E_c (V cm^{-1}) and low paraelectric to ferroelectric transition temperature (T_c in range of 10–120 K). However, in two recent reports, croconic acid[3b] and dehydroabietylamine-based Schiff bases[3c] have shown exceptional FE properties (P_s ~ 20–60 μC cm^{-2}). Recently an H-bonding driven all-organic two-component FE system[4] and a metal–ligand based design[5] have been highly successful. Interestingly, a module-based design strategy has also been extensively applied with other all-organic materials *e.g.*, semiconductors,[6a,b] FE liquid crystals,[6c,d] NLO materials,[6e] gels,[6f–h] and receptors.[6i] Such modular approach has an immense potential to achieve the elusive RT ferroelectricity, high spontaneous polarization and low E_c.

Herein, we report the first modular design strategy coupled with supramolecular[7] self-assembly approach which leads to ferroelectricity in AOSC crystalline solids as well as for the first time in organic nano-architectures. We could achieve spontaneous polarization at RT which is three orders of magnitude higher than the well-known AOSC FE materials.

As a proof of principle, we chose four modules to perform the following explicit functions and integrated them to a single-component FE material. *Module* A: a nitroaniline-based donor–π-acceptor (D–π-A) unit to attain spontaneous polarization due to its high dipole moment and ability to undergo π–π interactions.[8] *Module* B: an enantiomerically pure steroid unit to aid in polar ordering and facilitate self-assembly *via* van der Waals interaction.[9] *Module* C: H-bonding units for driving self-assembly process and *Module* D: a spacer unit capable of adjusting and error-proofing the packing between successive layers (Scheme 1a and b).

Compounds **1**, **2** and **3** were synthesized and thoroughly characterized by several analytical techniques (see ESI†).

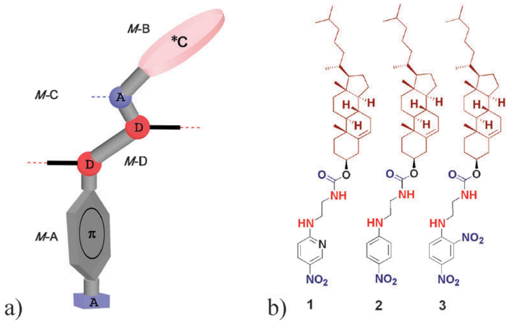

Scheme 1 (a) *M*-A, *M*-B (*C, chiral unit), *M*-C and *M*-D, are the various modules; (b) Structure of molecules.

---

[a] *Supramolecular & Material Chemistry Lab, School of Physical Sciences, JNU, New Delhi, 110067, India. E-mail: m_pritam@mail.jnu.ac.in; Fax: 91 11 26717537; Tel: 91 11 2673 8772*
[b] *School of Physical Sciences, JNU, New Delhi, 110067, India*
[c] *Department of Physics, IIT Delhi, 110016, India*
[d] *Polymer Science Unit, IACS, Kolkata, 700032, India*
[e] *X-Ray Crystallography: Department of Chemistry, Nanoscience Center, University of Jyväskylä, 40014, JYU. E-mail: kari.t.rissanen@jyu.fi*

† Electronic supplementary information (ESI) available: Experimental details, synthesis and characterization. CCDC 822459. For ESI and crystallographic data in CIF or other electronic format see DOI: 10.1039/c1cc12398j

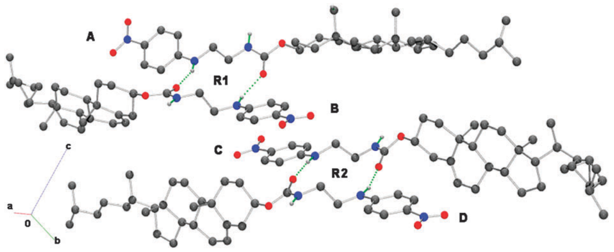

Fig. 1 X-Ray crystal structure of compound **2**, showing the H-bonded rings, π–π stacking and steroid–steroid supramolecular interactions.

The strong tendency of **1**, **2** and **3** to form self-assembled nano-architectures in a variety of solvents had posed a major challenge in growing single crystals. However, after more than a year of rigorous endeavour we have been able to grow ~1 cm long single crystals consistently as well as accomplish nano-architectures of **2** (page S9†).

Compound **2** crystallizes‡ in the non-centrosymmetric and polar space group $P1$ which is one of the ten polar point groups (C_1, C_s, C_2, C_{2v}, C_3, C_{3v}, C_4, C_{4v}, C_6 and C_{6v}) necessary for ferroelectricity to occur. The crystal lattice is constructed from two individual pairs of **2**, which are held together *via* four NH···O=C hydrogen bonds (N···O distances of 2.89/2.94 and 2.92/2.95 Å for the dimer A/B and C/D, respectively) (Fig. 1). These four N–H···O H-bonds result in the formation of two 14-membered supramolecular rings R_1 and R_2. These supramolecular interactions further propagate utilizing the four *n*-propanol solvent molecules which form H-bonds with the three amide H-atoms or the nitro group of the adjacent molecules (SI 1†). These pairs (A/B and C/D) form a pseudo-symmetric tetramer, through π–π interaction of the nitro-phenyl moieties with centroid-to-centroid distance of 3.82 Å and steroid–steroid van der Waals interactions ranging from 3.5 to 4.5 Å. Interestingly, the nitro-phenyl rings make an angle of 8° and the phenyl planes are tilted by 0.023 Å (SI 2†).

Compounds **1** and **3** produced stable crystalline materials. It becomes clearly evident from the X-ray crystal structure of **2** that each of the four modules (the π-ring, steroid moiety, H-bonding units and the spacer) execute their predicted roles. Similarity of the key modules in **1–3** and the molecular lengths (2.86–2.90 Å) from the optimized geometry points to a similar packing arrangements in the bulk. Circular dichroism (CD) spectroscopy showed well-defined positive CD signals for **1–3** which also confirms a similar polar ordering in all of these compounds (SI 3–4†).

We further ascertained the polar ordering in these compounds by performing second harmonic generation (SHG) measurements applying the Kurtz–Perry method using the fundamental 1064 nm light of a Q-switched Nd:YAG laser.[10] SHG efficiencies of **1**, **2** and **3** were found to be ~0.10, 0.11 and 0.05 times, respectively, that of KH_2PO_4 (KDP) (Table 1, see ESI†). Therefore, the SHG activity unequivocally confirms polar ordering in **1–3**.

To verify the ferroelectricity at RT, the polarization (P)–electric field (E) hysteresis curves of crystalline solid samples were determined (in the form of pellets) using a FE tester. Fig. 2 shows the P–E hysteresis loop, a typical FE feature for compound **1**. At an electric field of 10 kV cm^{-1}, P_s of 0.614 μC cm^{-2} was obtained as estimated by extrapolation of the P *vs.* E curves; P_r of 0.265 μC cm^{-2} and E_c of 3.67 kV cm^{-1} was determined with the field E sweeping back to zero. Compounds **2** and **3** also showed similar P–E loops at RT *e.g.*, **2** showed P_s, P_r and E_c of 0.511 μC cm^{-2}, 0.128 μC cm^{-2} and 2.44 kV cm^{-1} (SI 5–7, Table 2†).

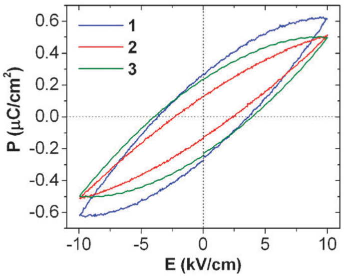

Fig. 2 Electric hysteresis loops at RT of **1**, **2** and **3** in the form of pellets recorded on a ferroelectric tester (model Precision Premier II) made by Radiant Technologies, Inc.

The highly attractive low E_c values (3-4 kV cm^{-1}) of **1–3** indicate a low energy barrier in reorienting the dipoles. This is because of the favourable supramolecular H-bonding and stacking interactions as is evident from the crystal structure of **2**. In comparison, vinylidene fluoride[11] a well-known FE organic copolymer shows extremely large E_c of 500–1200 kV cm^{-1} as it faces large steric barriers in reorienting dipoles. In addition a sizeable P_r value (remnant polarization at $E = 0$) in **1–3** reflects the fact that a definite angle between the molecular dipoles exists as can be clearly seen in the crystal structure of **2**. Similarly, the remnant dipoles reorient and undergo saturation polarization even at 0.31 kV (discussed later) demonstrating the efficient tunable nature of these supramolecular interactions.

Further, we evaluated the FE hysteresis properties of **1** (Fig. 3) and **2**, **3** as a function of applied voltages (SI 5–7†). Electric hysteresis loops are formed at voltages as low as 0.31 kV with P_s, P_r and E_c values of 0.124 μC cm^{-2}, 0.041 μC cm^{-2} and 0.70 kV cm^{-1}. As the voltage is increased up to 3.1 kV, P_s, P_r and E_c values increase uniformly to 1.24 μC cm^{-2}, 0.57 μC cm^{-2} and 7.56 kV cm^{-1}, respectively.

The P_s value obtained for **1** at 1.56 kV is more than three orders of magnitude higher than for well-known AOSC FE solid materials like benzil[3d] and tricyclohexylmethanol,[3e] three-fold higher than 1,6-bis(2,4-dinitrophenoxy)-2,4-hexadiyne (DNPH)[3f] and trichloroacetamide (TCAA)[3g] and two-fold higher than Rochelle salt.

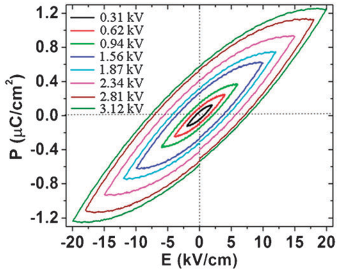

Fig. 3 Electric hysteresis loops at RT of **1** in the form of pellets at different applied voltages, recorded on a ferroelectric tester (model Precision Premier II) made by Radiant Technologies, Inc.

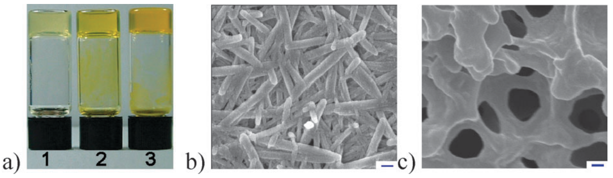

Fig. 4 (a) Organogels of **1**, **2** and **3** formed in various organic solvents; (b) and (c) nano-architectures formed by xerogels of **2** and **3**, respectively. Scale bar represents 100 nm.

Dielectric measurements of **1**, gave a value of 7.4 at RT, which is 85% and 64% higher than DNPH and TCAA, respectively. These measurements further revealed a sharp transition at 105 °C, due to the crystalline to cholesteric phase transition of the cholesteryl moiety (SI 9†).

It is worthwhile to consider that *P–E* loops can have some contribution from the *leakage* current.[12a] However, large values of P_s implies that leakage current, even if present, can be neglected as in the case with improper ferroelectricity in spin frustrated systems.[12b] We therefore measured the magnitude of leakage current and ascertained that the origin of the ferroelectricity in this material is due to the spontaneous polarization switching and is not due to the leakage of charges arising from the conduction. The leakage current measurement at RT of **1–3** show current densities of $1.06–1.83 \times 10^{-6}$ A cm^{-2} for an applied field of 10 kV cm^{-1} (SI 10†). These leakage current density values are comparable or lower than for known FE materials.[12c]

Furthermore, successful assimilation of FE properties in the nano-domain would result in a wide range of innovative materials.[13] Although there has been much research toward inorganic FE nano-materials, to the best of our knowledge, there are as yet no reports for the organic counterparts. To realize ferroelectricity in the nano-architectures the self-assembly properties of **1–3** were studied in a range of organic solvents. Compounds **1–3** formed thermo-reversible supramolecular networks in a broad range of common organic solvents (Fig. 4a, Table 4†).

SEM images (Fig. 4) revealed well-defined nano-architectures such as nanorods, porous sheets, *etc.* in the xerogels (SI 11†). As a representative example, we examined the FE properties of the nano-architectures formed by **3**, which clearly exhibits a *P–E* hysteresis loop at room temperature having P_s, P_r and E_c values of 0.498 μC cm^{-2}, 0.234 μC cm^{-2} and 3.95 kV cm^{-1}, respectively at 1.25 kV (SI 8†). This new approach therefore readily allows us to integrate FE property for the first time in all-organic nano-architectures.

To conclude, we have demonstrated the first applications of a modular design approach combined with supramolecular self-assembly to realize ferroelectricity in AOSC solids and for the first time in all-organic nano-architectures constituted from stable organogels. This approach has led to ~1 cm long FE crystals as well as nano-materials with the same molecule. We therefore believe that this new and general strategy should lead to many more innovative all-organic FE materials.

We thank DST for financial support and the Academy of Finland (KR: proj. no. 212588 and 218325). We thank Prof. P. K. Das and Mr Ravindra Pandey, IISC Bangalore, India for the SHG measurements and AIRF, JNU, New Delhi, India for the 500 MHz NMR, IR and CD facilities

Notes and references

‡ *Crystal data* for **2**: $4C_{36}H_{55}N_3O_4{\cdot}4C_3H_8O$, M = 2615.70, triclinic, space group $P1$, a = 12.9772(3), b = 14.3714(2), c = 22.6800(6) Å, α = 73.075(1), β = 79.981(1), γ = 69.560(1)°, V = 3779.5(1) Å^3, Z = 1, MoKα radiation (λ = 0.71073 Å), T = 123.0(1) K, μ = 0.075 mm^{-1}. Brucker-Nonius Kappa-APEXII diffractometer, 27 543 reflections, 13 227 independent (R_{int} = 0.0401), and 10 668 observed reflections [$I \geq 2\sigma(I)$], 1726 refined parameters, R = 0.06, $wR2$ = 0.13.

1 (*a*) S. J. Kang, I. Bae, Y. J. Park, T. H. Park, J. Sung, S. C. Yoon, K. H. Kim, D. H. Choi and C. Park, *Adv. Funct. Mater.*, 2009, **19**, 1609; (*b*) R. C. G. Naber, K. Asadi, P. W. M. Blom, D. M. De Leeuw and B. de Boer, *Adv. Mater.*, 2009, **21**, 1; (*c*) R. Schroeder, L. A. Majewski and M. Grell, *Adv. Mater.*, 2004, **16**, 633; (*d*) F. Kagawa, S. Horiuchi, M. Tokunaga, J. Fujioka and Y. Tokura, *Nat. Phys.*, 2010, **6**, 169; (*e*) G. Rogez, N. Viart and M. Drillon, *Angew. Chem., Int. Ed.*, 2010, **49**, 1921.

2 (*a*) S. E. Park, S. Wada, L. E. Cross and T. Shrout, *J. Appl. Phys.*, 1999, **86**, 2746; (*b*) E. Sawaguchi, *J. Phys. Soc. Jpn.*, 1953, **8**, 615.

3 For single-component organic ferroelectric solids, see: (*a*) J. Valasek, *Phys. Rev.*, 1921, **17**, 475; (*b*) S. Horiuchi, Y. Tokunaga, G. Giovannetti, S. Picozzi, H. Itoh, R. Shimano, R. Kumai and Y. Tokura, *Nature*, 2010, **463**, 789; (*c*) Y. Sui, D.-S. Liu, R.-H. Hu and H.-M. Chen, *J. Mater. Chem.*, 2011, DOI: 10.1039/c0jm03461d; (*d*) J. Sapriel, A. Boudou and A. Perigaud, *Phys. Rev. B*, 1979, **19**, 1484; (*e*) P. Szklarz and G. Bator, *J. Phys. Chem. Solids*, 2005, **66**, 121; (*f*) P.-B. Gruner and E. Dormann, *J. Phys.: Condens. Matter*, 1992, **4**, 5599; (*g*) Y. Kamishima, Y. Akishige and M. Hashimoto, *J. Phys. Soc. Jpn.*, 1991, **60**, 2147.

4 For two-component organic ferroelectric solids, see: (*a*) S. Horiuchi and Y. Tokura, *Nat. Mater.*, 2008, **7**, 357; (*b*) S. Horiuchi, R. Kumai and Y. Tokura, *Chem. Commun.*, 2007, 2321.

5 For organic–inorganic hybrid ferroelectric solids: (*a*) T. Okubo, R. Kawajiri, T. Mitani and T. Shimoda, *J. Am. Chem. Soc.*, 2005, **127**, 17598; (*b*) Q. Ye, Y.-M. Song, G.-Xi. Wang, K. Chen, D.-W. Fu, P. W. H. Chan, J.-s. Zhu, S. D. Huang and R.-G. Xiong, *J. Am. Chem. Soc.*, 2006, **128**, 6554; (*c*) W.-W. Zhou, J.-T. Chen, G. Xu, M.-S. Wang, J.-P. Zou, X.-F. Long, G.-J. Wang, G.-C. Guo and J.-S. Huang, *Chem. Commun.*, 2008, 2762; (*d*) W. Zhang, R.-G. Xiong and S. D. Huang, *J. Am. Chem. Soc.*, 2008, **130**, 10468.

6 For organic-based semiconductors, FE LCs, NLO materials, gels and receptors, see: (*a*) D. Braga and G. Horowitz, *Adv. Mater.*, 2009, **21**, 1473; (*b*) H. E. Katz, A. J. Lovinger, C. Kloc, T. Siegrist, W. Li, Y.-Y. Lin and A. Dodabalapur, *Nature*, 2000, **404**, 478; (*c*) S. T. Lagerwall, *Ferroelectric and Antiferroelectric Liquid Crystals*, Wiley-VCH, Weinheim, 1999; (*d*) W. Weissflog, G. Pelzl, H. Kresse, U. Baumeister, K. Brand, M. W. Schroder, M. G. Tamba, S. Findeisen-Tandel, U. Kornek, S. Stern, A. Eremin, R. Stannarius and J. Svoboda, *J. Mater. Chem.*, 2010, **20**, 6057; (*e*) B. J. Coe, *Chem.–Eur. J.*, 1999, **5**, 2464; (*f*) S. Banerjee, R. K. Das and U. Maitra, *J. Mater. Chem.*, 2009, **19**, 6649; (*g*) D. K. Smith, *Chem. Soc. Rev.*, 2009, **38**, 684; (*h*) N. Fujita, P. Mukhopadhyay and S. Shinkai, *Annu. Rev. Nano Res.*, 2006, **1**, 385; (*i*) P. Mal, B. Breiner, K. Rissanen and J. R. Nitschke, *Science*, 2009, **324**, 1697.

7 J.-M. Lehn, *Supramolecular Chemistry: Concepts and Perspectives*, Wiley-VCH, Weinheim, 1995.

8 P. Mukhopadhyay, P. K. Bharadwaj, G. Savitha, A. Krishnan and P. K. Das, *Chem. Commun.*, 2000, 1815.

9 Example of a steroid-thiophene based module: S.-i. Kawano, N. Fujita and S. Shinkai, *Chem.–Eur. J.*, 2005, **11**, 4735.

10 S. K. Kurtz and T. T. Perry, *J. Appl. Phys.*, 1968, **39**, 3798.

11 K. Noda, K. Ishida, A. Kubono, T. Horiuchi, H. Yamada and K. Matsushige, *J. Appl. Phys.*, 2003, **93**, 2866.

12 (*a*) R. Meyer and R. Waser, *Appl. Phys. Lett.*, 2005, **86**, 142907; (*b*) A. K. Singh, S. D. Kaushik, Brijesh Kumar, P. K. Mishra, A. Venimadhav, V. Siruguri and S. Patnaik, *Appl. Phys. Lett.*, 2008, **92**, 132910; (*c*) S. Fujisaki, H. Ishiwara and Y. Fujisaki, *Appl. Phys. Lett.*, 2007, **90**, 162902.

13 S. Mornet, C. Elissalde, O. Bidault, F. Weill, E. Sellier, O. Nguyen and M. Maglione, *Chem. Mater.*, 2007, **19**, 987.